PUBLICATION IV

Adaptation and failure of pancreatic beta cells in murine models with different degrees of metabolic syndrome

In: Desease Models & Mechanisms 2009.
Vol. 2, pp. 582–592.

RESEARCH ARTICLE

Disease Models & Mechanisms 2, 582-592 (2009) doi:10.1242/dmm.003251
Published by The Company of Biologists 2009

Adaptation and failure of pancreatic β cells in murine models with different degrees of metabolic syndrome

Gema Medina-Gomez[1,4,*], Laxman Yetukuri[2], Vidya Velagapudi[2], Mark Campbell[1], Margaret Blount[1], Mercedes Jimenez-Linan[3], Manuel Ros[1], Matej Orešič[2] and Antonio Vidal-Puig[1,*]

SUMMARY

The events that contribute to the expansion of β-cell mass and enhanced β-cell function in insulin-resistant states have not been elucidated fully. Recently, we showed that β-cell adaptation failed dramatically in adult, insulin-resistant POKO mice, which contrasts with the appropriate expansion of β cells in their *ob/ob* littermates. Thus, we hypothesised that characterisation of the islets in these mouse models at an early age should provide a unique opportunity to: (1) identify mechanisms involved in sensing insulin resistance at the level of the β cells, (2) identify molecular effectors that contribute to increasing β-cell mass and function, and (3) distinguish primary events from secondary events that are more likely to be present at more advanced stages of diabetes. Our results define the POKO mouse as a model of early lipotoxicity. At 4 weeks of age, it manifests with inappropriate β-cell function and defects in proliferation markers. Other well-recognised pathogenic effectors that were observed previously in 16-week-old mice, such as increased reactive oxygen species (ROS), macrophage infiltration and endoplasmic reticulum (ER) stress, are also present in both young POKO and young *ob/ob* mice, indicating the lack of predictive power with regards to the severity of β-cell failure. Of interest, the relatively preserved lipidomic profile in islets from young POKO mice contrasted with the large changes in lipid composition and the differences in the chain length of triacylglycerols in the serum, liver, muscle and adipose tissue in adult POKO mice. Later lipotoxic insults in adult β cells contribute to the failure of the POKO β cell. Our results indicate that the rapid development of insulin resistance and β-cell failure in POKO mice makes this model a useful tool to study early molecular events leading to insulin resistance and β-cell failure. Furthermore, comparisons with *ob/ob* mice might reveal important adaptive mechanisms in β cells with either therapeutic or diagnostic potential.

INTRODUCTION

The common forms of insulin-resistant type 2 diabetes typically involve an early phase characterised by insulin resistance, increased insulin secretion and a progressive expansion of β-cell mass. In response to insulin resistance, the islet machinery is challenged to secrete sufficient insulin to maintain euglycaemia. This requires robust adaptation that causes metabolic stress or an allostatic load on the physiological mechanisms that control insulin secretion and β-cell mass proliferation (Stumvoll et al., 2003). At some point, probably as a consequence of genetic vulnerability to metabolic stress, the balance between impaired insulin signalling and increased secretion of insulin fails, leading to hyperglycaemia and dyslipidaemia. These toxic metabolic disturbances increase the allostatic load on the system, ultimately causing a major collapse of the adaptive mechanisms and β-cell function (Stumvoll et al., 2003).

Studies performed in states of frank diabetes that aim to identify mechanisms involved in β-cell failure typically fail to distinguish early pathogenic mechanisms from either adaptive homeostatic responses or secondary pathogenic effects. In some cases, the same adaptive mechanism might exert opposite metabolic effects depending on how far advanced the β-cell failure is. This indicates that the mechanisms that provide an initial, positive, adaptive physiological response might become toxic at later stages when acting at high intensity and/or for extended periods of time. This concept is known as hormesis. For example, although the short-term exposure of islets to fatty acids promotes insulin secretion (Prentki et al., 2002; Roduit et al., 2004), chronic exposure to, and/or high concentrations of, fatty acids leads to β-cell failure (Prentki and Corkey, 1996; Bollheimer et al., 1998; Prentki et al., 2002). Similarly, there is evidence that reactive oxygen species (ROS), which are traditionally considered to be agents of molecular stress and damage (Brownlee, 2003; Lowell and Shulman, 2005), might, at small doses and for relatively short periods of time, provide a physiological signal that couples oxidation of glucose to insulin secretion (Li et al., 2006). This specific example is known as mitohormesis or mitochondrial hormesis (Schulz et al., 2007). Our hypothesis is that, in response to insulin resistance, specific responses in pancreatic β cells acutely improve their capacity to secrete insulin and trigger the expansion of β-cell mass. Although in the short term these adaptive mechanisms are efficient at maintaining carbohydrate homeostasis, when they are activated chronically, the same mechanisms might result in an excessive allostatic load that, ultimately, leads to collapse of the metabolic regulatory networks that control insulin secretion. Accumulating evidence indicates that diagnostic and therapeutic interventions at this late stage, when the homeostasis of the β-cell functional network is already lost, are inefficient, hence our focus on the early stages of the evolutive process where the dynamics of the

[1]University of Cambridge Metabolic Research Laboratories, Institute of Metabolic Science, Addenbrooke's Hospital, Cambridge CB2 0QQ, UK
[2]VTT Technical Research Centre of Finland, Tietotie 2, Espoo, P.O. Box1500, FIN-02044 VTT, Finland
[3]Department of Histopathology, Addenbrooke's Hospital, University of Cambridge, Cambridge, CB2 0QQ
[4]Present address: Departamento de Bioquímica, Fisiología y Genética Molecular, Universidad Rey Juan Carlos, Facultad de Ciencias de la Salud, Avda. de Atenas s/n, 28922 Alcorcón, Madrid, Spain
*Authors for correspondence (e-mail: gema.medina@urjc.es; ajv22@cam.ac.uk)

functional network can still be recognised and potentially reversed.

We recently generated a murine model, the POKO mouse, which was obtained by crossing a peroxisome proliferator-activated receptor gamma 2 (PPARγ2) knockout (KO) mouse into a genetically obese, insulin-resistant *ob/ob* background (Medina-Gomez et al., 2007). POKO and *ob/ob* mice have a similar positive energy balance (hyperphagia and energy dissipation), but because POKO mice lack PPARγ2 they are unable to expand adipose tissue and, as a result, they become lipotoxic and markedly more insulin resistant than their *ob/ob* littermates. By the age of 16 weeks, POKO mice show severe β-cell failure and hyperglycaemia. Another difference between the two mouse models is the lack of expansion of β cells in POKO mice, which contrasts with the markedly increased expansion of β-cell mass in insulin-resistant *ob/ob* littermates. Of interest, 4-week-old *ob/ob* and POKO mice have a similar islet number and morphology, which allowed us to investigate the mechanisms that might predict subsequent differences in metabolic profiles and expansion of β-cell mass in the two models.

The aim of our study was to investigate the early molecular regulatory networks that might account for the later differences in β-cell mass and function in insulin-resistant *ob/ob* and POKO mice. We speculated that these studies should validate the young POKO mouse as a model that could be used to study the events leading to β-cell failure and that would be suitable for future systems biology studies. This experimental paradigm also offers the possibility of identifying novel key events and molecular effectors that are involved in the adaptation of β cells to insulin resistance. Here, we show that isolated islets from mice as young as 4-5 weeks old reveal signs of inappropriate adaptive β-cell function and lipid signalling. Also, we provide evidence that other pathogenic effectors that are observed characteristically in advanced stages of disease, such as increased ROS production, inflammation, macrophage infiltration and endoplasmic reticulum (ER) stress, are already present at 4 weeks of age, which indicates their involvement in early pathogenic changes. However, our data also indicate that whereas these pathogenic mechanisms are present in β cells from early stages, they do not predict the rapid development of hyperglycaemia in POKO mice. Our data also indicate that the altered lipid composition of islets is a relatively late event in the context of lipotoxicity, which is preceded by lipid changes in the serum, liver, adipose tissue and muscle.

RESULTS

Differences in β-cell mass and function in *ob/ob* and POKO mice

We have reported previously that, in contrast to *ob/ob* mice, POKO mice do not expand their β-cell mass in response to insulin resistance (Medina-Gomez et al., 2007). As a result, adult POKO mice suffer metabolic collapse associated with severe β-cell failure that evolves over a relatively short period of 16 weeks. This contrasts with the robust expansion of β cells and the milder metabolic disturbances that are observed in *ob/ob* littermate controls, despite their marked obesity and insulin resistance. Interestingly, at the age of 4 weeks, the morphology of islets from POKO and *ob/ob* mice was indistinguishable, with the staining for insulin and glucagon being similar in both types of mice (Medina-Gomez et al., 2007).

Our initial studies in isolated islets from 4-week-old mice revealed that, at a low glucose concentration (2.5 mM), basal insulin secretion is maintained in POKO and *ob/ob* mice when compared with wild-type (WT) controls (Fig. 1A). Insulin secretion after 25 mM of glucose was stimulated significantly, but to a similar extent, in the insulin-resistant *ob/ob* and POKO mice. This indicates that, at this early age, the differences in insulin secretory defects between POKO and *ob/ob* mice are not established fully.

To validate the POKO model, we initially investigated the expression of genes involved in β-cell proliferation in young (5-week-old) C57BL/6 female WT, PPARγ2 KO, *ob/ob* and POKO mice. Insulin receptor substrate 2 (IRS2) (Fig. 1B) has been shown previously to be a key mediator of β-cell proliferation and to exert a protective role against β-cell glucotoxicity (Choudhury et al., 2005; Wang et al., 2005; Cantley et al., 2007). Our results in isolated islets from 5-week-old mice showed that, at this early stage, the amount of mRNA encoding IRS2 increased equally in *ob/ob* and POKO mice compared with WT and PPARγ2 KO mice. Similar results were obtained with staining for Ki67 (Fig. 1C), another marker of proliferation, which increased by a similar extent in β cells from *ob/ob* and POKO mice islets compared with WT and PPARγ2 KO controls. Despite these similar changes, we identified an important cell proliferation marker, cyclin D1, which is impaired selectively in the POKO mice. There is a greater increase in the expression of cyclin D1 in islets from *ob/ob* mice than in islets from POKO mice (although the expression in both of these genotypes is higher than in lean WT and PPARγ2 littermates) (Fig. 1B). Together, our results indicate that, compared with WT and PPARγ2 KO mice, proliferative programmes are activated in both *ob/ob* and POKO islets, even at this early stage, in response to insulin resistance. Furthermore, our results also highlight selective defects in cell proliferative genes in islets from POKO mice, which might indicate a subsequent failure of proliferation. Of interest, gene expression analysis in 5-week-old C57BL/6 female mice also revealed decreased levels of PPARγ1 in isolated islets from PPARγ2 KO and POKO mice, whereas the level of mRNA encoding PPARγ1 was maintained in *ob/ob* islets (Fig. 1B). From this, we speculated that the differences between *ob/ob* and POKO mice might be apparent in processes that are regulated by PPARγ (see below).

Markers of β-cell function that are associated with adaptation to insulin resistance are not apparent in islets from POKO mice

We undertook a systematic evaluation of the steps involved in coupling glucose concentration to insulin secretion. First, we investigated whether markers of glucose transport into islets are altered in POKO islets compared with the islets of other genotypes studied. Glut2 is the major glucose transporter involved in glucose uptake in islets, and is under the regulatory control of the pancreatic and duodenal homeobox 1 transcription factor (PDX1) (Lebrun et al., 2005). Glut2 is considered to be a surrogate of the state of differentiation of β cells. In agreement with this, we found that the expression levels of the mRNAs encoding both Glut2 and PDX1 are higher in islets from *ob/ob* mice, but that these increases were not present in POKO mice, which show similar expression levels to WT and PPARγ2 KO mice (Fig. 2A).

Next, we investigated the expression of genes involved in glucose intermediary metabolism, which is thought to be essential for

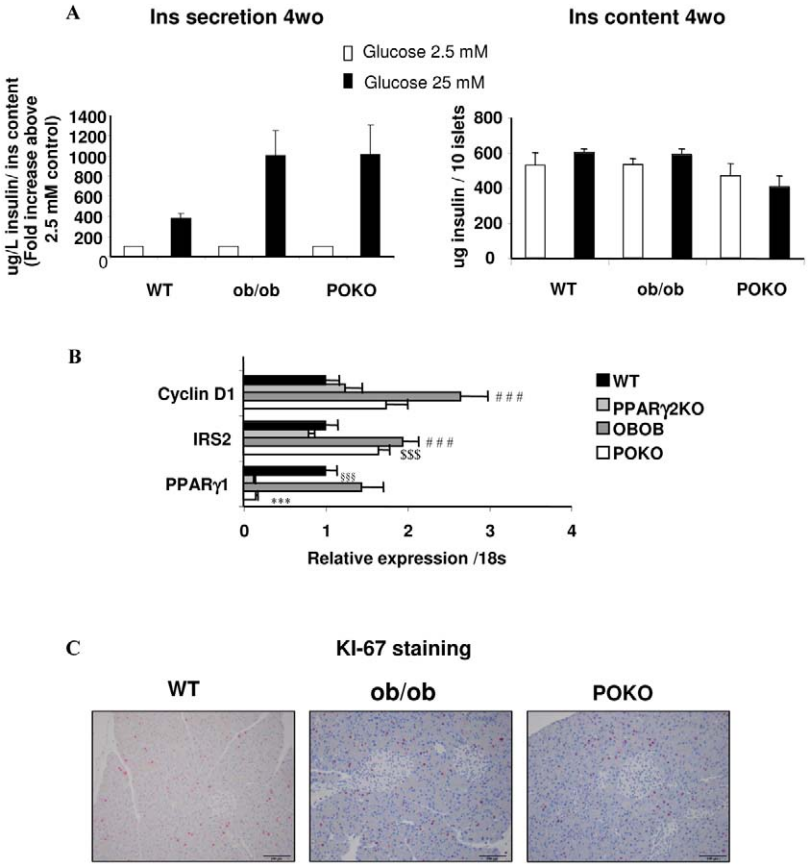

Fig. 1. β-cell function and proliferation in *ob/ob* and POKO mice. (A) Insulin secretion from islets isolated from WT, *ob/ob* and POKO mice in response to either 2.5 mM (white bars) or 25 mM (black bars) of glucose. Triplicate samples of ten different islets were obtained from each mouse (n=3-6 mice per genotype). For each sample, insulin release was normalised to insulin content and the fold increase in insulin above the 2.5 mM control mice was recorded. (B) Islet mRNA levels from different genes from 5-week-old female WT, PPARγ2 KO, *ob/ob* and POKO mice (n=8-11 mice per genotype). $^{###}P$<0.001 WT vs *ob/ob*; $^{§§§}P$<0.001 PPARγ2 KO vs WT; $^{$$$}P$<0.001 POKO vs PPARγ2 KO; $^{***}P$<0.001 POKO vs *ob/ob*. (C) Immunohistochemical analysis of Ki67 in the pancreas from 4-week-old male WT, *ob/ob* and POKO mice (n=5). Bars, 100 μm.

coupling glucose sensing to insulin release in β cells (Chen et al., 1994a; Chen et al., 1994b; Liu et al., 2002). An interesting difference between both young *ob/ob* and POKO mice was seen in the expression of mRNA encoding glucokinase (GK), which is upregulated by PPARγ agonists in β cells (Kim et al., 2002). In our studies, GK mRNA is increased in islets from *ob/ob* mice but not from POKO mice, in which expression levels remained comparable to WT and PPARγ2 KO mice (Fig. 2A). Expression of the gene pyruvate carboxylase (PCX), which is another target gene of PPARγ (Jitrapakdee et al., 2005), is decreased in PPARγ2 KO islets. As expected, the level of mRNA encoding PCX is also significantly decreased in islets from POKO mice compared with *ob/ob* mice (Hasan et al., 2008).

Compensation for insulin resistance requires a concomitant increase in insulin biosynthesis (Melloul et al., 2002). Our results indicate that, at the age of 4 weeks, both *ob/ob* and POKO mice can increase insulin gene expression to a level that is similar to WT mice. However, despite preserved expression of the insulin gene, transcription factors involved in insulin biosynthesis, such as v-maf musculoaponeurotic fibrosarcoma oncogene homologue A (MafA) (Olson et al., 1993; Hagman et al., 2005), are reduced in islets from PPARγ2 KO and POKO mice compared with WT and *ob/ob* mice (Fig. 2A).

Dysregulation of fatty acid metabolism in islets in young POKO mice

The mechanisms by which free fatty acids (FFAs) amplify glucose-induced insulin secretion have not been elucidated fully. Nevertheless, increased cytosolic malonyl-coenzyme A (CoA) that arises from glucose and de novo lipogenesis can act through AMP-activated protein kinase (AMPK)/malonyl-CoA pathways to limit fatty acid oxidation (Roduit et al., 2004). Interestingly, at these early stages, the levels of mRNA encoding sterol regulatory element-binding protein 1c (SREBP1c) are already increased in islets from *ob/ob* mice compared with WT, PPARγ2 KO and POKO mice. Of interest, POKO mice failed to show an increase in SREBP1c mRNA levels compared with *ob/ob* islets (Fig. 2B). However, at this stage, there were still no differences between *ob/ob* and POKO islets in their levels of expression of the mRNAs encoding acetyl-CoA carboxylase (ACC, also known as ACACA) or carnitine palmitoyltransferase 1 (CPT1) (Fig. 2B).

We have shown previously that the adult 16-week-old POKO islets contain a higher concentration of ceramides than *ob/ob* islets (Medina-Gomez et al., 2007). Here, we investigated whether defects in lipid metabolism were already present in islets at 4-5 weeks of age. Although we observed a trend, there were no statistically significant changes in lipid composition among the four genotypes of mice, as determined by analysis of variance (ANOVA) that was adjusted for multiple hypotheses (Fig. 3A). The levels of expression of mRNA encoding acid sphingomyelinase (ASM, SMPD1), an enzyme involved in generating ceramides from sphingomyelin, were increased in islets from both *ob/ob* and POKO mice compared with WT mice, although expression was higher in the *ob/ob* mice than in the POKO mice (Fig. 2B). Also, there were no significant changes in de novo ceramide synthesis

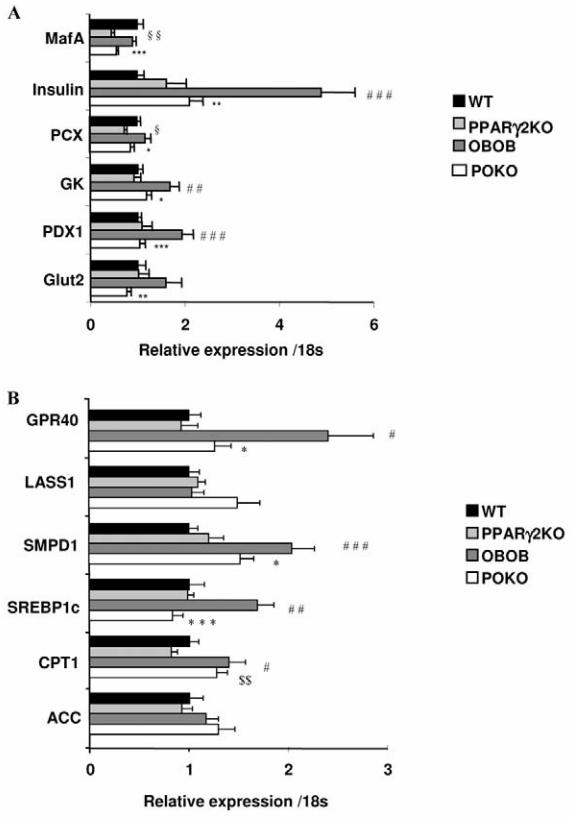

Fig. 2. Islet gene expression of glucose and lipid metabolism genes. (A) Islet gene expression from 5-week-old female WT, *ob/ob*, PPARγ2 KO and POKO mice (*n*=8-11 mice per genotype). (B) Islet gene expression of lipid metabolism genes from 5-week-old female WT, *ob/ob*, PPARγ2 KO and POKO mice (*n*=8-11 mice per genotype). $^{\#}P<0.05$, $^{\#\#}P<0.01$, $^{\#\#\#}P<0.001$ WT vs *ob/ob*; $^{\S}P<0.05$, $^{\S\S}P<0.01$ PPARγ2 KO vs WT; $^{\S\S}P<0.01$ POKO vs PPARγ2 KO; $^{*}P<0.05$, $^{**}P<0.01$, $^{***}P<0.001$ POKO vs *ob/ob*.

among the four genotypes, although there was a trend towards higher expression of ceramide synthase 1 (LASS1) in POKO islets compared with WT, PPARγ2 KO and *ob/ob* islets, which is in line with the increased levels of ceramides that were detected in older mice. Furthermore, expression of the gene encoding the G-protein-coupled receptor GPR40, a membrane receptor activated by lipids and involved in lipotoxicity (Itoh et al., 2003; Itoh and Hinuma, 2005), was higher in islets from *ob/ob* mice compared with WT, PPARγ2 KO and POKO mice (Fig. 2B). Our data indicate that, at this early age, islets from *ob/ob* and POKO mice are relatively protected from the accumulation of reactive toxic lipid species.

Early lipidomic changes in metabolically relevant organs in young POKO mice

Next, we investigated whether the relatively preserved lipid composition in POKO islets can also be observed in other metabolically relevant organs. In contrast to β cells, a multivariate analysis revealed large differences in the lipid profiles of serum, liver, adipose tissue and muscle (see below) in WT, PPARγ2 KO, *ob/ob* and POKO mice at the age of 4 weeks.

As expected from the hypertriglyceridaemia that was observed at 4 weeks of age, the serum from POKO mice had high levels of short-, medium- and long-chain triacylglycerols (TAGs), and high levels of short- and medium-chain phosphatidylcholine (PC) lipid species compared with the other genotypes studied (Fig. 3B). Interestingly, the levels of long-chain TAGs in the serum from young *ob/ob* mice were lower than in WT and PPARγ2 KO mice.

Lipidomic analyses of the liver also revealed differences in lipid profiles at 4 weeks of age (Fig. 4), with an increase in short- and medium-chain diacylglycerols (DAGs) and TAGs in *ob/ob* and POKO livers compared with WT livers; there was also a slight increase in these lipids in PPARγ2 KO livers. We also observed enrichment in unsaturated long-chain TAGs in POKO and *ob/ob* livers. Polyunsaturated long-chain TAGs remained at similar low levels in both POKO and *ob/ob* livers when compared with WT and PPARγ2 KO mice (Fig. 4). Although the ceramide concentration was similar in PPARγ2 KO, POKO and *ob/ob* livers, it was higher than in WT mice at this early age. The levels of medium-chain PCs also increased in livers from *ob/ob* and POKO mice compared with WT and PPARγ2 KO mice.

With respect to adipose tissue, at this stage, POKO and *ob/ob* mice had similar levels of short-, medium- and long-chain TAGs (see supplementary dataset). Unlike in the liver, the concentration of polyunsaturated long-chain TAGs with a high number of double bonds was higher in adipose tissue from POKO and *ob/ob* mice than from WT and PPARγ2 KO mice. The ceramide concentration was also increased to similar levels in the POKO and *ob/ob* genotypes.

Lipidomic analysis of muscle showed an increased concentration of short- and medium-chain TAGs in *ob/ob* mice compared with the other genotypes (Fig. 5). Conversely, muscle from POKO and PPARγ2 KO mice contained more long-chain TAGs than WT and *ob/ob* muscles. Compared with WT and PPARγ2 KO mice, muscles from *ob/ob* and POKO mice were enriched in ceramides, which correlated with the extent of the increased levels of lysoPCs.

Oxidative stress is not an early mechanism linked to β-cell failure in POKO mice

The toxic effects of increased ROS are proposed to mediate β-cell failure (Maedler et al., 2002; Kaneto et al., 2005). Here, we investigated whether the excessive toxicity of ROS is an early pathogenic mechanism that determines the divergence in β-cell phenotype between *ob/ob* and POKO mice. The production of ROS, which was measured using CM-H_2DCFDA, a cell-permeable indicator of ROS, revealed no differences between POKO and *ob/ob* islets (Fig. 6A). Uncoupling protein 2 (UCP2) is a mitochondrial carrier that is activated by ROS and reduces insulin secretion. We observed no differences in the levels of mRNA encoding UCP2 in islets, which supports the notion that ROS do not contribute to the early stages of β-cell failure in the POKO mouse (supplementary material Fig. S1A). Furthermore, the expression of mRNA encoding ROS scavengers that are typically induced during oxidative stress, such as manganese superoxide dismutase (MnSOD), is unchanged in islets from POKO and *ob/ob* mice compared with WT mice. The expression of other intracellular antioxidant enzymes such as glutathione peroxidase 1 (GPX-1) and glutathione reductase 1 (GSR-1) were also similar in the four genotypes, which further indicates that, at this age, differences in oxidative stress are unlikely

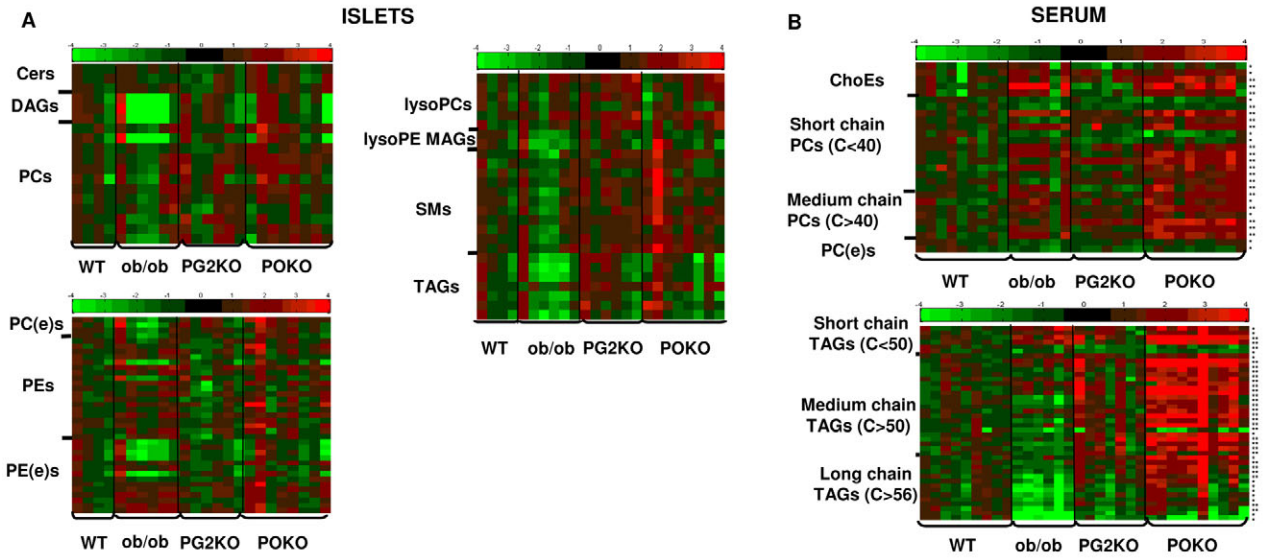

Fig. 3. Lipidomic profiling of islets and serum. Lipidomic profiling of islets (A) and serum (B) from 4-week-old male WT, PPARγ2 KO (PG2KO), *ob/ob* and POKO mice (n=5-8 mice per genotype). Lipids with ANOVA P values of $P<0.05$ are shown. Lipid variable P values: $^{*}P<0.05$, $^{**}P<0.01$. Abbreviations: Cers, ceramides; ChoEs, cholesteryl esters; DAGs, diacylglycerols; lysoPCs, lysophosphatidylcholines; lysoPE MAGs, lysophosphatidylethanolamine monoacylglycerols; PCs, phosphatidylcholines; PC(e)s, ether-linked phosphatidylcholines; PEs, phosphatidylethanolamines; PE(e)s, ether-linked phosphatidylethanolamines; SMs, sphingomyelins; TAGs, triacylglycerols.

to be a main determinant of the rapid evolution of β-cell failure in pancreatic islets of the POKO mice.

Macrophage infiltration, islet inflammation and fibrosis in POKO islets

Next, we investigated whether inflammation was present in islets at this early stage and, therefore, whether this might be an early pathogenic mechanism responsible for the accelerated β-cell failure in islets of POKO mice. At 4 weeks of age, the expression of the macrophage markers CD68 and F4/80 is increased in islets from *ob/ob* and POKO mice compared with WT and PPARγ2 KO mice, indicating that macrophage infiltration in islets is an early event in the development of the metabolic syndrome. However, at this early age, macrophage infiltration of islets per se does not predict the subsequent evolution towards β-cell failure in POKO mice. In support of this, we observed no differences in the expression of interleukin (IL)-6 and tumour necrosis factor (TNF)α mRNA in islets (Fig. 6B) and/or in the level of fibrosis, as assessed by Picrosirius Red staining in 4-week-old mice from the four genotypes (supplementary material Fig. S2). Similarly, there was no evidence of increased apoptosis in islets using a TUNEL assay (Fig. 6C), and no difference in the expression of Bcl2 in POKO, *ob/ob*, WT and PPARγ2 KO mice (Fig. 6B). Together, these data indicate that although *ob/ob* and POKO mice show some proinflammatory changes at 4 weeks of age, these changes do not predict the future divergence in β-cell failure in these mice.

ER stress is not an early pathogenic mechanism leading to β-cell failure in POKO mice

Metabolically overstretched β cells make high demands on the ER for the biosynthesis of insulin (Nakatani et al., 2005). As these demands become chronic, the biosynthesis of insulin might overload the protein-folding capacity of the ER and so play a role in the development of β-cell failure (Kaneto et al., 2005; Nakatani et al., 2005; Wellen and Hotamisligil, 2005). We investigated whether early differences in ER stress markers could predict the subsequent evolution of β-cell function in *ob/ob* and POKO mice. Initially, we assessed X-box binding protein 1 (XBP1), a transcription factor that is downstream of inositol-requiring protein 1 (IRE1) and that is a transmembrane protein in the ER, which functions as a sensor and transducer of ER stress (Eizirik et al., 2008). The mRNA levels of the precursor form of XBP1 (unspliced) and the active (spliced) form, which is formed by an IRE1-mediated splicing reaction following ER stress, were similar in the four genotypes (supplementary material Fig. S1B). Moreover, an ER overload leads to apoptosis through the induction of the C/EBP homologous protein Chop (Huang et al., 2007; Laybutt et al., 2007; Marchetti et al., 2007). Although the mRNA expression level of Chop is increased in both *ob/ob* and POKO mice at 5 weeks of age compared with WT and PPARγ2 KO mice, this increase is lower in POKO mice than in *ob/ob* mice. However, expression of the ER chaperone glucose-regulated protein 78 (GRP78) is similar in *ob/ob* and POKO mice compared with WT and PPARγ2 KO mice (supplementary material Fig. S1B). This result indicates that although incipient ER stress occurs in the early stages of β-cell compensation, it alone cannot be used to predict the course of development of β-cell expansion and failure.

DISCUSSION

Our goal was to characterise the early events and molecular factors leading to β-cell adaptation and failure in the context of obesity and insulin resistance. For this, we took advantage of a recently generated mouse model, the POKO mouse, which was obtained by crossing a PPARγ2 KO mouse with an *ob/ob* mouse, as described previously (Medina-Gomez et al., 2007). This study focuses on the early events that lead to severe metabolic syndrome. Our hypothesis

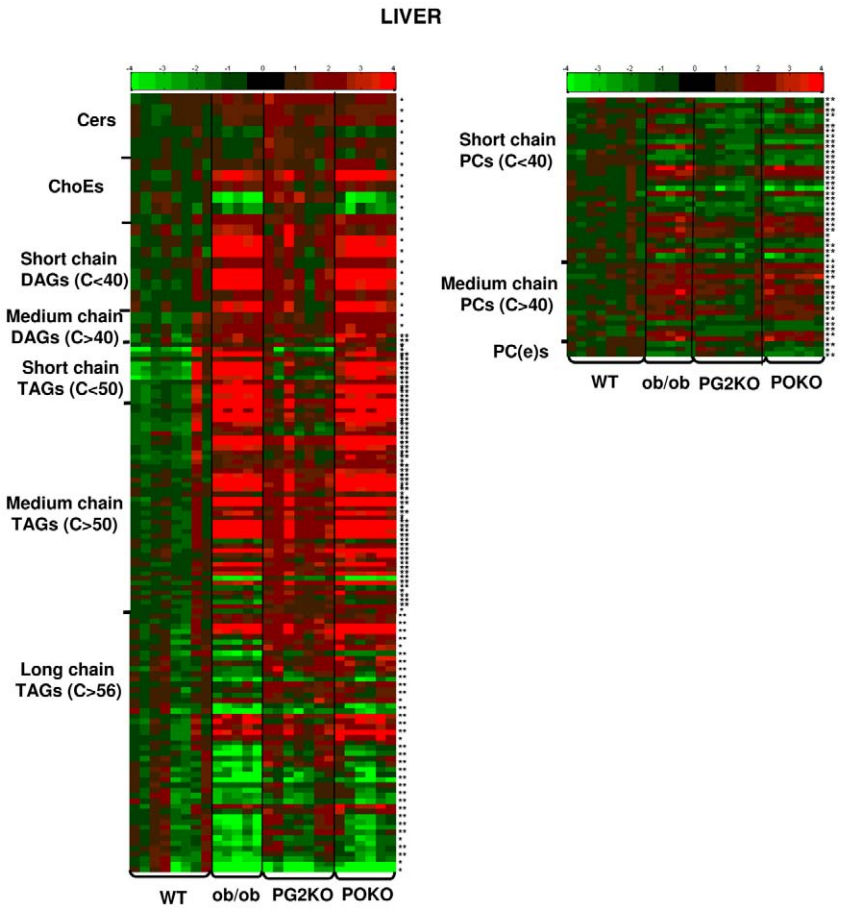

Fig. 4. Lipidomic profiling of the liver. Lipidomic profiling of the liver from 4-week-old male WT, PPARγ2 KO (PG2KO), *ob/ob* and POKO mice (*n*=5-8 mice per genotype). Lipids with ANOVA *P* values of $P<0.05$ are shown. Lipid variable *P* values: $*P<0.05$, $**P<0.01$.

is that the early stages of disease might provide important novel clues in the pathogenesis of metabolically induced β-cell failure and diabetes.

Here, we show that differences in metabolic stress are detected as early as 4-5 weeks of age, as illustrated by the differences observed between *ob/ob* and POKO islets at a time when the mass and functional qualities of their β cells are apparently conserved. Previous studies addressing this subject have faced the problem of discriminating primary pathogenic mechanisms from secondary toxic hits, or even from protective secondary allostatic responses that maintain the metabolic homeostasis of the system. Here, we focused on early events in an attempt to unravel the differences that, at an early age, could be predictive of β-cell failure. The strength of our experimental design is based on comparing two mouse models that have different degrees of severity and kinetics of β-cell failure and on using PPARγ2 KO and WT mice, which are not insulin resistant and have normal β-cell function, as controls. Our data indicate that, despite their apparently normal β-cell morphology and function, metabolic and genetic differences in young *ob/ob* and POKO mice differentially affect β-cell function and lipid metabolism in response to insulin resistance. We observed that other well-established mechanisms that are associated with β-cell failure, such as increased ROS production, inflammation, macrophage infiltration and ER stress, are already present at this early age. As these proinflammatory mechanisms are equally apparent in POKO and *ob/ob* mice, it is possible that the main difference between β-cell failure in POKO and *ob/ob* mice might be related to decreased resistance to stress. Our data also indicate that these measures cannot be used to predict β-cell failure, at least in our models.

To validate the POKO mouse as a model of β-cell failure, and to validate its potential use in translational studies, we initially characterised specific candidate mechanisms that have been suggested previously to be involved in β-cell failure in humans. As indicated above, our results represent an in-depth characterisation of the early metabolic events in β cells in two mouse models that both eventually develop metabolic syndrome, although with differing severity. As such, their comparative analysis offers the opportunity of identifying predictors of the metabolic syndrome development and severity. One model, the POKO mouse, develops severe metabolic syndrome owing to positive energy balance, impaired adipose tissue expandability and accelerated β-cell failure (Medina-Gomez et al., 2007). The *ob/ob* mouse is a genetic model of positive energy balance that results from increased food intake and decreased energy expenditure. Adipose tissue expansion is not impaired in this model; nevertheless, the mice develop the metabolic syndrome. One of the most puzzling, and interesting, findings of the initial characterisation of adult POKO mice was their inability to expand β-cell mass, a response that is typical of other insulin-resistant strains, such as their *ob/ob* littermates. Another interesting observation is that, despite the marked differences in β-cell mass

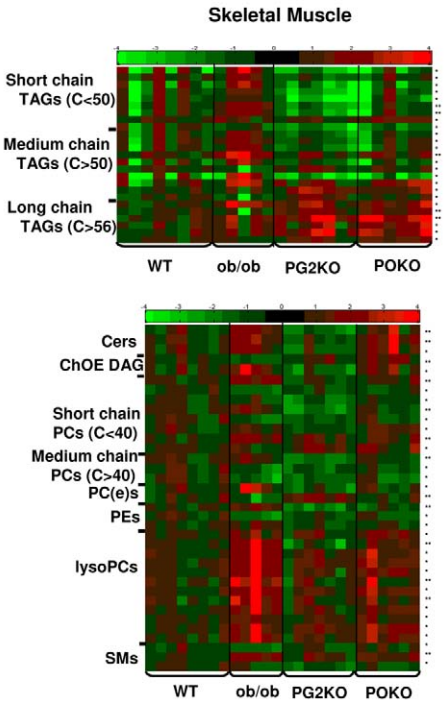

Fig. 5. Lipidomic profiling of skeletal muscle. Lipidomic profiling of skeletal muscle from 4-week-old male WT, PPARγ2 KO (PG2KO), *ob/ob* and POKO mice (*n*=5-8 mice per genotype). Lipids with ANOVA *P* values of $P<0.05$ are shown. Lipid variable *P* values: $*P<0.05$, $**P<0.01$.

in adult mice, β-cell mass and function in younger (4-5 weeks old) POKO and *ob/ob* mice are indistinguishable, which indicates that this might be an interesting time at which to explore early mediators of the subsequent divergent response.

Our results confirm that, at 4 weeks of age, POKO and *ob/ob* mice have a similar β-cell mass (Medina-Gomez et al., 2007), and conserved basal and stimulated insulin secretion. Conservation of the insulin secretory capacity of *ob/ob* and POKO islets indicates that, at this stage, islets from these models are relatively healthy. This led us to speculate that the differences observed at this stage should be enriched in primary adaptations in comparison to the more likely secondary adaptive and/or toxic responses that become apparent in advances stages of the disease.

Our results confirm that it is possible to work efficiently with such small islets and to detect signs of metabolic stress in this tissue. We observed upregulation of IRS2 mRNA, a key mediator of β-cell proliferation that protects β cells against glucotoxicity. We also observed upregulation of mRNA encoding Ki67, which is another marker of cell proliferation that stains from the early to mid-G1 phase of the cell cycle through to mitosis. Given the adaptive increase in β-cell mass to maintain euglycaemia in the presence of marked insulin resistance, the increased expression of cyclin D1 in *ob/ob* islets was not unexpected. Although this may appear paradoxical in leptin-deficient mice, as cyclin D1 has been shown to be a target of leptin (Saxena et al., 2007), it indicates that other specific regulators of cyclin D1 regulate β-cell mass expansion. Our data also indicate that induction of cyclin D1 in β cells might be regulated, in part, by PPARγ under conditions of either overnutrition or metabolic stress. However, this hypothesis is challenged by the observation that cyclin D1 is not altered in islets from PPARγ2 KO mice, even though pharmacological activation of PPARγ decreases cyclin D1 expression in vitro (Yin et al., 2001; Koga et al., 2003). Alternatively, it has been suggested that agonist-mediated inhibition of cell growth might be independent of PPARγ activation (Bae et al., 2003). Despite the opposing roles of leptin and PPARγ in modulating β-cell mass, our data indicate that robust alternative mechanisms are able to expand β-cell mass appropriately under conditions of increased metabolic demands. These studies also lead us to speculate that a systems biology approach to studying POKO islets might be a useful way to identify these mechanisms. In any case, defining the role of cyclin D1 in coupling β-cell expansion to insulin resistance is an important subject for subsequent studies.

Our data are sufficiently sensitive to detect specific metabolic disturbances in islets from young mice. For example, Glut2, an important transporter required for glucose uptake in islets, and its main upstream regulator PDX1, are induced in islets from *ob/ob* mice. In POKO islets, however, expression of Glut2 and PDX1 is similar to that observed in WT islets, which could be considered similar to unstressed physiological levels. In addition to compromised glucose uptake into islets from POKO mice, the early steps of glucose metabolism are likely to be affected, as indicated by selective defects in GK and PCX expression in islets (Hasan et al., 2008). As suggested above, these genes appear to be bona fide PPARγ targets because GK is regulated by thiazolidinediones in β cells (Kim et al., 2002), and our group has evidence that PCX is a target of PPARγ action (Jitrapakdee et al., 2005). This reinforces the idea that the POKO model might be enriched in defects in PPARγ-dependent mechanisms of β-cell homeostasis. Similarly, these data indicate that PPARγ targets might be important for the adaptation of β cells to insulin resistance and nutritional stress. As expected, expression of the gene encoding insulin is increased in islets from 5-week-old *ob/ob* and POKO mice compared with non-insulin-resistant PPARγ2 KO and WT islets. However, it might be argued that the level of upregulation in POKO mice is inappropriately low considering that these mice are more insulin resistant than *ob/ob* mice. Gene expression analysis further supports the concept of inappropriate adaptation to metabolic stress in POKO mice, as indicated by the blunted transcriptional upregulation of MafA and PDX1 in POKO islets compared with the marked upregulation that was observed in *ob/ob* islets. Our studies of glucose sensing and fuel handling also distinguish between the severity of metabolic stress in the two models. When considered globally, islets from POKO mice showed inappropriate adaptations in β-cell function, and defects in proliferation markers and lipid signalling. Interestingly, compared with WT islets, the expression of metabolic genes in POKO islets was unchanged, with a profile that could be considered to be inappropriately normal for the severe metabolic stress.

Following our original data from adult POKO mice (Medina-Gomez et al., 2007), we sought to identify whether defects in fatty acid metabolism and lipotoxicity were already evident in islets from young POKO mice. The importance of the role of fatty acid metabolism in β-cell function is illustrated by the fact that FFAs amplify glucose-induced insulin secretion, although the mechanisms of this effect are far from being elucidated. It has

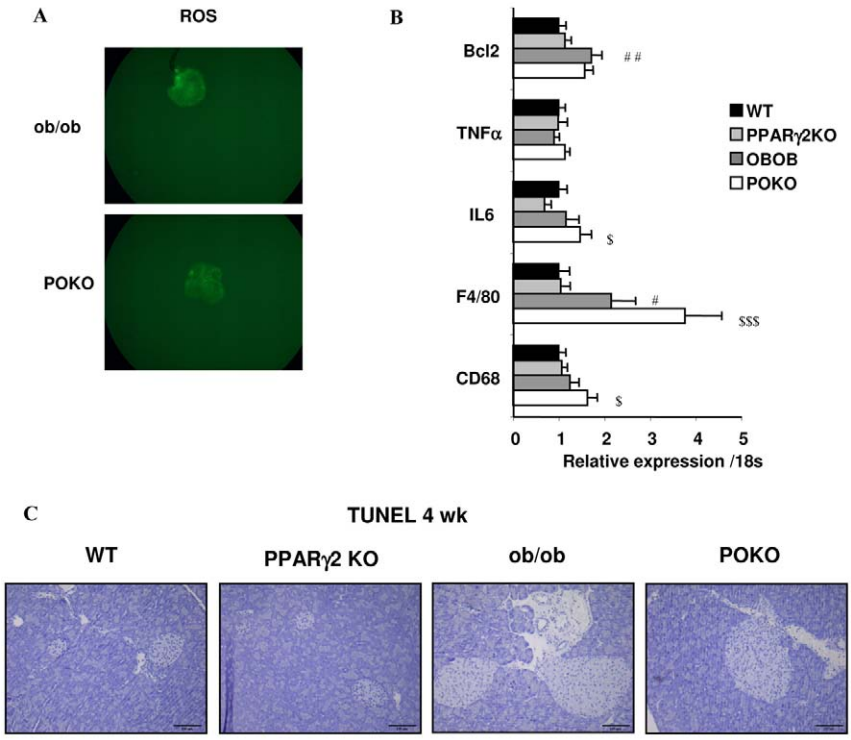

Fig. 6. Islet ROS production, gene expression and apoptosis in young mice. (A) ROS production was measured by CM-H_2DCFDA fluorescence, as described in the Methods. (B) Islet gene expression from 5-week-old female WT, *ob/ob*, PPARγ2 KO and POKO mice (n=8-11 mice per genotype). $^{\#}P<0.05$, $^{\#\#}P<0.01$ WT vs *ob/ob*; $^{\$}P<0.05$, $^{\$\$\$}P<0.001$ POKO vs PPARγ2 KO.
(C) Representative pancreatic sections showing apoptosis in WT, *ob/ob*, PPARγ2 KO and POKO mice, determined by TUNEL. Bars, 100 μm.

been suggested that inappropriate activation of AMPK/ACC/malonyl-CoA/CPT1 pathways might limit fatty acid oxidation and compromise β-cell function (Roduit et al., 2004). In young mice, there were no differences in the expression of ACC or CPT1 mRNA. However, even at this early stage, expression of the gene encoding SREBP1c was decreased in POKO islets compared with *ob/ob* islets. This is an interesting observation because there is evidence that excessive activation of SREBP1c reduces insulin secretion and genetically modified mouse models have indicated that SREBP1c has a physiological role in β cells (Yamashita et al., 2004; Takahashi et al., 2005; Shimano et al., 2007). Furthermore, recent evidence indicates that enhanced lipid synthesis that is mediated by SREBP1c-dependent genes might be required for the adaptive changes in islet gene expression and insulin secretion that occur at high glucose concentrations (Diraison et al., 2008). Induction of SREBP1c might, in our opinion, contribute to the hormetic effect of fatty acids on insulin secretion. In this regard, the increase in SREBP1c that was observed in *ob/ob* mice, compared with WT mice, might be an adaptation to promote lipogenesis in response to glucose levels; this adaptation seems to be missing in islets from POKO mice, despite similar challenging metabolic conditions.

We have also optimised a sensitive and sophisticated lipidomic platform that is sufficiently sensitive to characterise the small number of islets isolated from 4-week-old mice. Unlike in adult mice (Medina-Gomez et al., 2007), the lipid composition of islets from young POKO mice was unchanged when compared with the other genotypes. However, lipidomic analysis of other metabolically relevant tissues revealed important changes in lipid species in young animals. For example, livers from both POKO and *ob/ob* mice had similarly increased TAG levels, predominantly short- and medium-chain TAGs, at 4 weeks of age. A priori, we would expect POKO mice to accumulate more TAGs than *ob/ob* mice, particularly considering the decrease in adipose tissue expandability that is secondary to ablation of PPARγ2, and the severity of the metabolic disturbances (e.g. hyperlipidaemia) in POKO mice compared with the other genotypes. In this respect, the similarity between TAG accumulation in the livers of *ob/ob* and POKO mice is compatible with some degree of impaired TAG deposition in the POKO liver.

Another interesting finding comes from analysis of skeletal muscle from 4-week-old POKO mice; these data showed that the concentrations of short- and medium-chain TAGs increased by less than in skeletal muscle from *ob/ob* mice and were associated with an increased concentration of other lipid species, such as long-chain TAGs. This result agrees with the lipid profile observed in the POKO mouse at later stages. Of interest, the levels of ceramides and proinflammatory lysoPCs increased similarly in both *ob/ob* and POKO mice. Overall, our lipidomic studies suggest that the defective accumulation of TAGs and the resulting lipotoxicity in relevant metabolic tissues, coupled with accelerated β-cell failure and the relatively low levels of insulin, may contribute to the severity of the metabolic syndrome and the lipidomic profile observed in mature POKO mice. Our data also highlight qualitative and quantitative differences in organ-specific lipid networks and their contribution to insulin resistance. These lipidomic studies and, more specifically, the differences observed between the liver, serum and muscle, may also indicate the possibility of a hierarchical order of organs with respect to fat deposition and lipid-induced toxicity. In this respect,

our results indicate that, when adipose tissue storage becomes incompetent, islets are not the first tissue to be to be affected by lipid insult; it is more likely that the liver is the first organ to serve as a sink for fat.

Our analysis of the early mechanisms leading to β-cell adaptation and failure provide evidence that islet inflammation, ROS and ER stress, which are all alterations that are observed in the context of severe advanced apoptosis of β cells (Poitout and Robertson, 2002), are already present in islets from young POKO and *ob/ob* mice but not in islets from PPARγ2 KO and WT mice. However, we do not conclude that these proinflammatory mechanisms are predictive markers of either severity or the prognosis of β-cell failure. In our opinion, it is more likely that the primary mechanism, in this case the ablation of PPARγ, defines the vulnerability of the β cells to these pathogenic mechanisms.

In summary, we have characterised the early metabolic alterations in islets from *ob/ob* mice and compared them with islets of the more severely affected POKO mice, and then compared these to the changes in WT and PPARγ2 KO controls. Our results confirm that β cell studies at this early age are both feasible and sufficiently sensitive to identify altered processes, and to discriminate between different degrees of severity. Our results justify future systems biology studies to investigate the early stages of β-cell disease as a strategy to maximise the chances of identifying primary pathogenic mechanisms over secondary hits and allostatic changes. Our lipidomic approach reveals that the lipid profile of metabolically relevant organs changes during the course of the disease, and that these changes are specific to the particular organ. Taken together, our data support the concept that studies in young mouse models are informative; that *ob/ob* mice, and particularly the accelerated phenotype of POKO mice, provide good models to study the early mechanisms associated with β-cell failure; and that coupling studies in β cells with lipid analysis in other organs might provide important information about the chronology of lipid disturbances in specific organs in the context of lipotoxicity and the metabolic syndrome.

METHODS

Animal care

Animals were housed at a density of four animals per cage in a temperature-controlled room (20-22°C) with 12-hour light-dark cycles. Food and water were available ad libitum unless noted. All animal protocols used in this study were approved by the UK Home Office and the University of Cambridge.

Isolation and culture of pancreatic islets

The pancreas was injected, though the bile duct, with cold Hank's solution containing 0.4% (w/v) collagenase P (Roche Biochemicals). The pancreas was removed, digested for 8 minutes, and islets were collected by hand picking. Isolated islets were cultured overnight in cell medium (RPMI 1640 with 10% FBS, and penicillin and streptomycin), at 37°C, in 5% CO_2 in air. For insulin secretion studies or RNA extraction, islets were used on the day after isolation.

Insulin secretion studies

Insulin secretion from isolated islets (10 islets/well) was measured for 30 minutes at 37°C in incubations in Krebs-Ringer buffer, supplemented with 0.1% bovine serum albumin (BSA) as a carrier containing either basal (2.5 mM) or stimulatory (25 mM) glucose concentrations. The supernatants were assayed for insulin. Insulin content was extracted using a 95:5 ethanol:acetic acid solution. Insulin was measured using an electrochemical luminescence immunoassay from MesoScale Discovery (MSD) (Gaithersburg, MD). For these experiments, islets were isolated from several mice of each genotype. Thus, the data are the mean of separate experiments in which data were collected for each test solution from samples of 10 islets each. For each sample, insulin release was normalised to insulin content.

RNA preparation and real-time quantitative PCR

Total RNA was isolated from islets and tissue samples according to the manufacturer's instructions (RNAeasy kit, Qiagen). Real-time quantitative PCR was performed using a TaqMan 7900 (Abi), according to standard protocols.

Light microscopy and immunohistochemical analysis

Tissue samples for morphological and immunohistochemical analyses were prepared according to published protocols (Medina-Gomez et al., 2007). Morphometric analyses of pancreas sections were acquired using a digital camera and microscope (Olympus BX41), and cell areas were measured using AnalySIS software (Soft Imaging System). The antibodies used for immunohistochemistry were as follows: Ki67 staining was detected using streptavidin alkaline phosphatase (Zymed) at 1:2000 in TTBSA (Tris-Tyrode's buffer supplemented with BSA), and visualised with SigmaFast Fast Red TR/Naphthol AS-MX phosphate tablets. TUNEL staining slides were pretreated with Dako Real proteinase K for 5 minutes and then the staining was performed using Millipore's ApopTag peroxidase in situ apoptosis detection kit (Chemicon S7100), according to the manufacturer's instructions. For estimation of collagen deposition, slides were stained with Weigert's iron haematoxylin (made in-house) for 30 minutes, then briefly differentiated and counterstained with Picrosirius Red (Pioneer Research chemicals) for 1 hour, rapidly dehydrated, cleared, and mounted in Micromount.

Measurement of ROS production

To determine the production of ROS in whole islets, islets were loaded with 5 mol/l of CM-H_2DCFDA for 1 hour followed by three washes with fresh culture medium. ROS production was visualised on a fluorescent microscope equipped with a digital camera. One representative figure from three independent experiments with similar results is shown (Fig. 6A).

Lipid profiling

Serum samples (10 μl), tissue samples (about 20 mg for liver, white adipose tissue and skeletal muscle tissue) or islet samples were diluted with 0.9% NaCl (10 μl for serum and islets, 50 μl for tissue samples) and spiked with an internal standard reference compounds mixture (10 μl for serum and islets, 20 μl for tissue samples) (Laaksonen et al., 2006). The samples were subsequently extracted with chloroform:methanol (2:1) solvent (100 μl for serum, 90 μl for islets, 200 μl for tissue samples), homogenised with a glass rod, vortexed (1 minute for serum, 15 seconds for islets, 2 minutes for tissue samples), incubated at room temperature (1 hour for serum and tissue samples, 20 minutes for islets), and centrifuged at 7826 ***g***

TRANSLATIONAL IMPACT

Clinical issue

The earliest stages of type 2 diabetes are characterised by growing insulin resistance and increased insulin secretion from an expanding population of pancreatic β cells. In later stages, the β cells fail and, in the insulin-resistant environment, they cannot produce sufficient insulin to maintain blood glucose control. The ability to understand the crucial steps that precipitate diabetes and β-cell failure is hampered by limited mouse models for the early stages of the disease. Most models are examined after the failing of β cells, making it difficult to define the events leading to expansion and excessive insulin production by β cells, and their subsequent failure.

Results

Here, the authors define a mouse model for studying the early pathological changes that result from elevated fat levels or lipotoxicity. They use the POKO mouse, a mouse model obtained by crossing the insulin-resistant *ob/ob* mouse (which lacks leptin) with the peroxisome proliferator-activated receptor gamma 2 (PPARγ2) knockout mouse that lacks the nuclear receptor PPARγ2, which is known to have a role in adipogenesis. The POKO mouse becomes lipotoxic and more insulin resistant than the *ob/ob* mouse. Changes are found in the lipid profiles of POKO mice as young as 4 weeks of age and are associated already with changes in β-cell proliferation and function. At this early time, pathogenic effectors that characterise the advanced stages of disease can be observed. Lipidomic analysis of the β cells in pre-diabetic mice reveal that, compared with other metabolically relevant organs such as the liver, muscle or adipose tissue, these pancreatic cells are protected from lipid-induced toxicity at the early stages of disease. This suggests a hierarchical order of ectopic lipid accumulation in which β cells are protected initially, and establishes a model for understanding the early events leading to diabetes.

Implications and future directions

Previous models are limited in their ability to address issues about the early sensing of insulin resistance and the effectors that contribute to changes in β-cell mass and function. The authors suggest that these data establish a foundation for subsequent systems biology profiling studies to identify the mechanisms by which β cells initially sense insulin resistance and eventually fail from metabolic pressure. Further work should reveal the molecular effectors that increase β-cell mass and function in the early phase of diabetes and suggest biomarkers for early stages of the disease.

doi:10.1242/dmm.004499

for 3 minutes. From the separated lower phase, an aliquot was mixed with 10 ml of a labelled standard mixture (three stable isotope-labelled reference compounds), and a 1.0-ml injection was used for liquid chromatography-mass spectrometry (LC-MS) analysis. The sample order for analysis was established by randomisation. Lipid extracts were analyzed on a Q-ToF Premier mass spectrometer (Waters) combined with Acquity ultra-performance liquid chromatography (UPLC-MS) (Medina-Gomez et al., 2007) in ESI+ mode. Data processing was performed using the MZmine software (Katajamaa et al., 2006). The normalisation procedure for lipidomic data was as described previously (Laaksonen et al., 2006). Serum lipidomic data were normalised against the serum volume of samples, and lipidomic data from tissues were normalised against their tissue weights. Identification of lipid species was performed based on an internal database of a lipid library or, alternatively, by utilising the tandem mass spectrometry library.

Statistics

For lipidomic studies, an array view of lipid profiles reflected the changes relative to the mean intensity of molecular species within the WT group. One-way ANOVA was performed to investigate whether the mean intensities differed among the four genotypes. Lipids with ANOVA P values of $P<0.05$ were shown. The lipid variables with P values lying between $P<0.05$ and $P<0.01$ were marked with '*' and those with P values of $P<0.01$ were marked with '**'. The multivariate statistical data analyses were performed using Matlab (Mathworks) and the Matlab library PLS Toolbox (Eigenvector Research).

The rest of the results are given as the mean±S.E. (standard error). Statistical differences and interactions were evaluated through a two-way lack of leptin and lack of PPARγ2 factorial ANOVA. When statistically significant differences resulted at the interaction level, the Student's t-test was carried out to compare the effects. The differences were considered to be statistically significant at $P<0.05$.

ACKNOWLEDGEMENTS

We thank Keith Burling, Janice Carter and Daniel Hart for their work. We thank Sophie Gough, Maria Adams and Sergio Rodriguez-Cuenca for their comments on the writing of this manuscript. We thank the funding bodies that have supported the research within our laboratory leading to this work: Diabetes UK, FP6 Hepadip, and the MRC career establishment award and MRC CORD. Manuel Ros is a recipient of a Salvador de Madariaga fellowship from MEC, Spain. Deposited in PMC for release after 6 months.

COMPETING INTERESTS

The authors declare no competing financial interests.

AUTHOR CONTRIBUTIONS

G.M.-G. and A.V.-P. conceived and designed the experiments; G.M.-G., V.V., L.Y., M.C., M.J.-L., M.B. and M.R. performed the experiments; G.M.-G., V.V., L.Y. and M.O. analyzed the data; G.M.-G. and A.V.-P. wrote the paper.

SUPPLEMENTARY MATERIAL

Supplementary material for this article is available at
http://dmm.biologists.org/lookup/suppl/doi:10.1242/dmm.003251/-/DC1

Received 24 March 2009; Accepted 8 July 2009.

REFERENCES

Bae, M. A., Rhee, H. and Song, B. J. (2003). Troglitazone but not rosiglitazone induces G1 cell cycle arrest and apoptosis in human and rat hepatoma cell lines. *Toxicol. Lett.* **139**, 67-75.

Bollheimer, L. C., Skelly, R. H., Chester, M. W., McGarry, J. D. and Rhodes, C. J. (1998). Chronic exposure to free fatty acid reduces pancreatic beta cell insulin content by increasing basal insulin secretion that is not compensated for by a corresponding increase in proinsulin biosynthesis translation. *J. Clin. Invest.* **101**, 1094-1101.

Brownlee, M. (2003). A radical explanation for glucose-induced beta cell dysfunction. *J. Clin. Invest.* **112**, 1788-1790.

Cantley, J., Choudhury, A. I., Asare-Anane, H., Selman, C., Lingard, S., Heffron, H., Herrera, P., Persaud, S. J. and Withers, D. J. (2007). Pancreatic deletion of insulin receptor substrate 2 reduces beta and alpha cell mass and impairs glucose homeostasis in mice. *Diabetologia* **50**, 1248-1256.

Chen, C., Bumbalo, L. and Leahy, J. L. (1994a). Increased catalytic activity of glucokinase in isolated islets from hyperinsulinemic rats. *Diabetes* **43**, 684-689.

Chen, C., Hosokawa, H., Bumbalo, L. M. and Leahy, J. L. (1994b). Mechanism of compensatory hyperinsulinemia in normoglycemic insulin-resistant spontaneously hypertensive rats. Augmented enzymatic activity of glucokinase in beta-cells. *J. Clin. Invest.* **94**, 399-404.

Choudhury, A. I., Heffron, H., Smith, M. A., Al-Qassab, H., Xu, A. W., Selman, C., Simmgen, M., Clements, M., Claret, M., Maccoll, G. et al. (2005). The role of insulin receptor substrate 2 in hypothalamic and beta cell function. *J. Clin. Invest.* **115**, 940-950.

Diraison, F., Ravier, M. A., Richards, S. K., Smith, R. M., Shimano, H. and Rutter, G. A. (2008). SREBP1 is required for the induction by glucose of pancreatic beta-cell genes involved in glucose sensing. *J. Lipid Res.* **49**, 814-822.

Eizirik, D. L., Cardozo, A. K. and Cnop, M. (2008). The role for endoplasmic reticulum stress in diabetes mellitus. *Endocr. Rev.* **29**, 42-61.

Hagman, D. K., Hays, L. B., Parazzoli, S. D. and Poitout, V. (2005). Palmitate inhibits insulin gene expression by altering PDX-1 nuclear localization and reducing MafA expression in isolated rat islets of Langerhans. *J. Biol. Chem.* **280**, 32413-32418.

Hasan, N. M., Longacre, M. J., Stoker, S. W., Boonsaen, T., Jitrapakdee, S., Kendrick, M. A., Wallace, J. C. and MacDonald, M. J. (2008). Impaired anaplerosis and insulin secretion in insulinoma cells caused by small interfering RNA-mediated suppression of pyruvate carboxylase. *J. Biol. Chem.* **283**, 28048-28059.

Huang, C. J., Lin, C. Y., Haataja, L., Gurlo, T., Butler, A. E., Rizza, R. A. and Butler, P. C. (2007). High expression rates of human islet amyloid polypeptide induce endoplasmic reticulum stress mediated beta-cell apoptosis, a characteristic of humans with type 2 but not type 1 diabetes. *Diabetes* **56**, 2016-2027.

Itoh, Y. and Hinuma, S. (2005). GPR40, a free fatty acid receptor on pancreatic beta cells, regulates insulin secretion. *Hepatol. Res.* **33**, 171-173.

Itoh, Y., Kawamata, Y., Harada, M., Kobayashi, M., Fujii, R., Fukusumi, S., Ogi, K., Hosoya, M., Tanaka, Y., Uejima, H. et al. (2003). Free fatty acids regulate insulin secretion from pancreatic beta cells through GPR40. *Nature* **422**, 173-176.

Jitrapakdee, S., Slawik, M., Medina-Gomez, G., Campbell, M., Wallace, J. C., Sethi, J. K., O'Rahilly, S. and Vidal-Puig, A. J. (2005). The peroxisome proliferator-activated receptor-gamma regulates murine pyruvate carboxylase gene expression in vivo and in vitro. *J. Biol. Chem.* **280**, 27466-27476.

Kaneto, H., Matsuoka, T. A., Nakatani, Y., Kawamori, D., Miyatsuka, T., Matsuhisa, M. and Yamasaki, Y. (2005). Oxidative stress, ER stress, and the JNK pathway in type 2 diabetes. *J. Mol. Med.* **83**, 429-439.

Katajamaa, M., Miettinen, J. and Oresic, M. (2006). MZmine: toolbox for processing and visualization of mass spectrometry based molecular profile data. *Bioinformatics* **22**, 634-636.

Kim, H. I., Cha, J. Y., Kim, S. Y., Kim, J. W., Roh, K. J., Seong, J. K., Lee, N. T., Choi, K. Y., Kim, K. S. and Ahn, Y. H. (2002). Peroxisomal proliferator-activated receptor-gamma upregulates glucokinase gene expression in beta-cells. *Diabetes* **51**, 676-685.

Koga, H., Harada, M., Ohtsubo, M., Shishido, S., Kumemura, H., Hanada, S., Taniguchi, E., Yamashita, K., Kumashiro, R., Ueno, T. et al. (2003). Troglitazone induces p27Kip1-associated cell-cycle arrest through down-regulating Skp2 in human hepatoma cells. *Hepatology* **37**, 1086-1096.

Laaksonen, R., Katajamaa, M., Paiva, H., Sysi-Aho, M., Saarinen, L., Junni, P., Lutjohann, D., Smet, J., Van Coster, R., Seppanen-Laakso, T. et al. (2006). A systems biology strategy reveals biological pathways and plasma biomarker candidates for potentially toxic statin-induced changes in muscle. *PLoS ONE* **1**, e97.

Laybutt, D. R., Preston, A. M., Akerfeldt, M. C., Kench, J. G., Busch, A. K., Biankin, A. V. and Biden, T. J. (2007). Endoplasmic reticulum stress contributes to beta cell apoptosis in type 2 diabetes. *Diabetologia* **50**, 752-763.

Lebrun, P., Montminy, M. R. and Van Obberghen, E. (2005). Regulation of the pancreatic duodenal homeobox-1 protein by DNA-dependent protein kinase. *J. Biol. Chem.* **280**, 38203-38210.

Li, X., Chen, H. and Epstein, P. N. (2006). Metallothionein and catalase sensitize to diabetes in nonobese diabetic mice: reactive oxygen species may have a protective role in pancreatic beta-cells. *Diabetes* **55**, 1592-1604.

Liu, Y. Q., Jetton, T. L. and Leahy, J. L. (2002). beta-cell adaptation to insulin resistance: increased pyruvate carboxylase and malate-pyruvate shuttle activity in islets of nondiabetic Zucker fatty rats. *J. Biol. Chem.* **277**, 39163-39168.

Lowell, B. B. and Shulman, G. I. (2005). Mitochondrial dysfunction and type 2 diabetes. *Science* **307**, 384-387.

Maedler, K., Sergeev, P., Ris, F., Oberholzer, J., Joller-Jemelka, H. I., Spinas, G. A., Kaiser, N., Halban, P. A. and Donath, M. Y. (2002). Glucose-induced beta cell production of IL-1beta contributes to glucotoxicity in human pancreatic islets. *J. Clin. Invest.* **110**, 851-860.

Marchetti, P., Bugliani, M., Lupi, R., Marselli, L., Masini, M., Boggi, U., Filipponi, F., Weir, G. C., Eizirik, D. L. and Cnop, M. (2007). The endoplasmic reticulum in pancreatic beta cells of type 2 diabetes patients. *Diabetologia* **50**, 2486-2494.

Medina-Gomez, G., Gray, S. L., Yetukuri, L., Shimomura, K., Virtue, S., Campbell, M., Curtis, R. K., Jimenez-Linan, M., Blount, M., Yeo, G. S. et al. (2007). PPAR gamma 2 prevents lipotoxicity by controlling adipose tissue expandability and peripheral lipid metabolism. *PLoS Genet.* **3**, e64.

Melloul, D., Marshak, S. and Cerasi, E. (2002). Regulation of insulin gene transcription. *Diabetologia* **45**, 309-326.

Nakatani, Y., Kaneto, H., Kawamori, D., Yoshiuchi, K., Hatazaki, M., Matsuoka, T. A., Ozawa, K., Ogawa, S., Hori, M., Yamasaki, Y. et al. (2005). Involvement of endoplasmic reticulum stress in insulin resistance and diabetes. *J. Biol. Chem.* **280**, 847-851.

Olson, L. K., Redmon, J. B., Towle, H. C. and Robertson, R. P. (1993). Chronic exposure of HIT cells to high glucose concentrations paradoxically decreases insulin gene transcription and alters binding of insulin gene regulatory protein. *J. Clin. Invest.* **92**, 514-519.

Poitout, V. and Robertson, R. P. (2002). Minireview: Secondary beta-cell failure in type 2 diabetes-a convergence of glucotoxicity and lipotoxicity. *Endocrinology* **143**, 339-342.

Prentki, M. and Corkey, B. E. (1996). Are the beta-cell signaling molecules malonyl-CoA and cystolic long-chain acyl-CoA implicated in multiple tissue defects of obesity and NIDDM? *Diabetes* **45**, 273-283.

Prentki, M., Joly, E., El-Assaad, W. and Roduit, R. (2002). Malonyl-CoA signaling, lipid partitioning, and glucolipotoxicity: role in beta-cell adaptation and failure in the etiology of diabetes. *Diabetes* **51 Suppl. 3**, S405-S413.

Roduit, R., Nolan, C., Alarcon, C., Moore, P., Barbeau, A., Delghingaro-Augusto, V., Przybykowski, E., Morin, J., Masse, F., Massie, B. et al. (2004). A role for the malonyl-CoA/long-chain acyl-CoA pathway of lipid signaling in the regulation of insulin secretion in response to both fuel and nonfuel stimuli. *Diabetes* **53**, 1007-1019.

Saxena, N. K., Vertino, P. M., Anania, F. A. and Sharma, D. (2007). Leptin-induced growth stimulation of breast cancer cells involves recruitment of histone acetyltransferases and mediator complex to CYCLIN D1 promoter via activation of Stat3. *J. Biol. Chem.* **282**, 13316-13325.

Schulz, T. J., Zarse, K., Voigt, A., Urban, N., Birringer, M. and Ristow, M. (2007). Glucose restriction extends Caenorhabditis elegans life span by inducing mitochondrial respiration and increasing oxidative stress. *Cell Metab.* **6**, 280-293.

Shimano, H., Amemiya-Kudo, M., Takahashi, A., Kato, T., Ishikawa, M. and Yamada, N. (2007). Sterol regulatory element-binding protein-1c and pancreatic beta-cell dysfunction. *Diabetes Obes. Metab.* **9 Suppl. 2**, 133-139.

Stumvoll, M., Tataranni, P. A., Stefan, N., Vozarova, B. and Bogardus, C. (2003). Glucose allostasis. *Diabetes* **52**, 903-909.

Takahashi, A., Motomura, K., Kato, T., Yoshikawa, T., Nakagawa, Y., Yahagi, N., Sone, H., Suzuki, H., Toyoshima, H., Yamada, N. et al. (2005). Transgenic mice overexpressing nuclear SREBP-1c in pancreatic beta-cells. *Diabetes* **54**, 492-499.

Wang, H., Kouri, G. and Wollheim, C. B. (2005). ER stress and SREBP-1 activation are implicated in beta-cell glucolipotoxicity. *J. Cell Sci.* **118**, 3905-3915.

Wellen, K. E. and Hotamisligil, G. S. (2005). Inflammation, stress, and diabetes. *J. Clin. Invest.* **115**, 1111-1119.

Yamashita, T., Eto, K., Okazaki, Y., Yamashita, S., Yamauchi, T., Sekine, N., Nagai, R., Noda, M. and Kadowaki, T. (2004). Role of uncoupling protein-2 up-regulation and triglyceride accumulation in impaired glucose-stimulated insulin secretion in a beta-cell lipotoxicity model overexpressing sterol regulatory element-binding protein-1c. *Endocrinology* **145**, 3566-3577.

Yin, F., Wakino, S., Liu, Z., Kim, S., Hsueh, W. A., Collins, A. R., Van Herle, A. J. and Law, R. E. (2001). Troglitazone inhibits growth of MCF-7 breast carcinoma cells by targeting G1 cell cycle regulators. *Biochem. Biophys. Res. Commun.* **286**, 916-922.